ARKIV FÖR FYSIK Band 18 nr 2

Communicated 13 April 1960 by O. Klein and E. Rudberg

The relativistic photoeffect at the *K*-shell threshold

By Bengt C. H. Nagel and Per O. M. Olsson

With 2 figures in the text

SUMMARY

The *K*-shell photoeffect is studied in the limit of zero kinetic energy of the outgoing photoelectron. The relativistic $(\alpha Z)^2$ corrections are obtained in the general case, and "exact" numerical calculations are performed for $Z=92$. The total cross section is reduced by 21 % (for $Z=92$), and the angular distribution is changed somewhat, compared to the non-relativistic results. Considerable electron polarization effects are obtained.

Introduction

In the preceding paper (Nagel, 1960, hereafter denoted by I), one of the present authors studied the *K*-shell photoeffect and derived expressions for the matrix elements to relative order αZ in a Coulomb field, using a final state wave function, exact to order $(\alpha Z)^2$. For heavy atoms this approximation is poor, and one has to use the exact expression for the final state wave function as a series of partial waves. The reaction amplitudes, in terms of which the photoelectric matrix elements were expressed in I, are then obtained in form of series expansions in radial multipole matrix elements, corresponding to a retardation expansion of the plane wave of the radiation field. The radial Coulomb matrix elements must in general be computed numerically, and as a large number of these matrix elements contribute, especially at higher energies, it is important to have suitable and rapidly convergent series expansions. This problem has been studied by one of us in a number of papers (Olsson, 1959; Olsson and Hultberg, 1959; the last paper will be denoted by II).

At the *K*-shell threshold, where the photon energy is equal to the binding energy of the *K*-electron, one should expect the expansions in multipole moments to converge rather rapidly, as the photon wavelength is then, even for heavy atoms, considerably larger than the radius of the *K*-orbit. The limiting form of the radial matrix elements has been derived in II in connection with a study of the internal conversion at low energies. In the internal conversion matrix elements the radiation field enters in the form of spherical Hankel functions, whereas in the photoeffect one has spherical Bessel functions. The results in II can then be taken over directly, our matrix elements being the real parts of those in II.

The radial matrix elements are then expressed in terms of a confluent hypergeometric function of two variables. For the computation of this function a rapidly convergent series in ordinary confluent hypergeometric functions can be used. We first derive the expressions for the reaction amplitudes to relative order $(\alpha Z)^2$ (the terms of order αZ vanish in this limit), and then also perform a numerical calculation for the case $Z=92$, taking into account transitions to final states up to and including the g-states.

1. The radial matrix elements in the zero energy limit

The relevant radial matrix elements are defined in I (3.8). We want to obtain analytic expressions for these matrix elements for a pure Coulomb field, especially in the limit $\beta=0$ ($\beta=v/c$, where v is the velocity of the photoelectron). This is the same problem as treated in II, except that we have spherical Bessel functions instead of spherical Hankel functions in the integrals. The normalization of the radial electron wave functions is also different in I and II; the functions used in I (3.8) are obtained from the corresponding bound and continuum functions $N_i \chi$ and $N_f \chi$ in II (11), (2), and (24) by multiplication with

$$\frac{a}{\sqrt{\pi}} t^{-1} \quad \text{and} \quad a\sqrt{\frac{2\pi}{\varepsilon p}}\, t^{-1}, \quad \text{respectively.} \tag{1.1}$$

Here $t=2ar$, $a=\alpha Z$; ε is denoted by E in II. We use in general the same notation as in I.

Our matrix elements can now be expressed in $\operatorname{Re} J_1$ and $\operatorname{Re} J_2$, II (13), (14), and (15). We then perform the transition to the limit $\beta=0$, see II (19). The final result is

$$\begin{aligned} &\lim_{p\to 0} p^{\frac{1}{2}} \int g_i f_\varkappa j_l(kr)\, r^2\, dr \\ &\quad = N\Big[H_7(\gamma_1+\gamma_\varkappa+l+1;\, l+\tfrac{3}{2}, 2\gamma_\varkappa;\, x_0, -2) \\ &\qquad + \frac{\gamma_1+\gamma_\varkappa+l+1}{\gamma_\varkappa(2\gamma_\varkappa+1)} H_7(\gamma_1+\gamma_\varkappa+l+2;\, l+\tfrac{3}{2}, 2\gamma_\varkappa+2;\, x_0, -2)\Big], \end{aligned} \tag{1.2}$$

$$\begin{aligned} &\lim_{p\to 0} p^{\frac{1}{2}} \int f_i g_\varkappa j_l(kr)\, r^2\, dr \\ &\quad = -N\Big[\frac{\varkappa-\gamma_\varkappa}{1+\gamma_1} H_7(\gamma_1+\gamma_\varkappa+l+1;\, l+\tfrac{3}{2}, 2\gamma_\varkappa;\, x_0, -2) \\ &\qquad + \frac{\varkappa+\gamma_\varkappa}{1+\gamma_1}\,\frac{\gamma_1+\gamma_\varkappa+l+1}{\gamma_\varkappa(2\gamma_\varkappa+1)} H_7(\gamma_1+\gamma_\varkappa+l+2;\, l+\tfrac{3}{2}, 2\gamma_\varkappa+2;\, x_0, -2)\Big], \end{aligned} \tag{1.3}$$

with
$$N=\frac{1}{8}\sqrt{\frac{2\pi(1+\gamma_1)}{\Gamma(2\gamma_1+1)}}\,2^{\gamma_1}\,\frac{\Gamma(\gamma_1+\gamma_\varkappa+l+1)\,2^{\gamma_\varkappa}}{\Gamma(2\gamma_\varkappa+1)}\,\frac{z^l}{\Gamma(l+\frac{3}{2})}, \tag{1.4}$$

$$z=\frac{a}{2(1+\gamma_1)}, \quad x_0=-z^2, \quad \gamma_\varkappa=\sqrt{\varkappa^2-a^2}.$$

$\varkappa$ (which is different from the $\varkappa$ used in I) here characterizes the final state, $\varkappa=l_f$ or $-l_f-1$.

H_7 is a confluent hypergeometric function in two variables, and can be expressed as a series of ${}_1F_1$ functions:

$$H_7(a;\, b, c;\, x, y)=\sum_{m=0}^{\infty}\frac{(a)_{2m}\,x^m}{(b)_m\,m!}\,{}_1F_1(a+2m;\, c;\, y), \tag{1.5}$$

with
$$(b)_n=b(b+1)\ldots(b+n-1), \quad (b)_0=1.$$

In the expressions I (3.7) we also need the asymptotic phases $\eta_\varkappa$; for the Coulomb field we have (cf. Olsson, 1959, pp. 137, 138, (22) and (23))

$$\eta_\varkappa=\tfrac{1}{2}\pi(l-\gamma_\varkappa)-\arg\Gamma(\gamma_\varkappa+i\,a/\beta)-\operatorname{arc\,tg}\frac{p(\varkappa-\gamma_\varkappa)}{a(\varepsilon-1)}, \quad (\varkappa=l \text{ or } -l-1). \tag{1.6}$$

The value of arc tg should be chosen in the interval $(0, \pi)$. In the limit $\beta=0$ (the arc tg then goes to $\frac{1}{2}\pi$) we get, using Stirling's formula for the Γ-function,

$$\lim_{\beta\to 0}(\eta_\varkappa+\varphi_0)=\tfrac{1}{2}\pi(l-2\gamma_\varkappa), \tag{1.7}$$

where
$$\varphi_0=a/\beta\,[\ln(a/\beta)-1]+\tfrac{1}{4}\pi \tag{1.8}$$

is infinite in the limit, but independent of $\varkappa$, so that it gives a common phase-factor to A, E, F, and G in I (3.7).

2. The reaction amplitudes including order $(\alpha Z)^2$

From the expressions for A, B, C, and D to first order in a, given in I ((5.3) to (5.6)), we get, if we let β go to zero and define

$$A'(\theta)=\lim_{\beta\to 0} i\exp(i\varphi_0)\,p^{\frac{1}{2}}A(\theta) \tag{2.1}$$

and so on, φ_0 as in (1.8), the following limiting values:

$$\left.\begin{aligned} A'(\theta)&=K\sin\theta\exp(-i\,a\cos\theta)\\ E'(\theta)&=F'(\theta)=G'(\theta)=0\end{aligned}\right\}, \tag{2.2}$$

with $K=8\pi\sqrt{2}\,e^{-2}$ ($e=$ basis of natural logarithms).

This gives the ordinary non-relativistic $\sin^2\theta\cos^2\phi$ angular distribution, no polarizations, and a total cross section (per K-electron)

$$\sigma_0=\frac{256\,\pi^2}{3\,e^4}\,\alpha\left(\frac{\hbar}{m\,c}\right)^2\frac{mc^2}{h\nu}=1.679\times10^{-22}\frac{m\,c^2}{h\,\nu}\ \mathrm{cm}^2. \tag{2.3}$$

We will now use the expansions I (3.7) and the limiting forms (1.2) and (1.3) of the radial matrix elements to derive expressions for the amplitudes $A'\ldots G'$ including order a^2. As z is of order a, this means that we must take into account all radial matrix elements containing $j_l(kr)$ with $l\leqslant 2$. The calculations are rather lengthy, but perfectly straightforward. For $l=1$ and 2 we can put $\gamma_1=1$ and $\gamma_\varkappa=|\varkappa|$ everywhere, both in the matrix elements and in the phase-factors $\exp(i\,\eta_\varkappa)$, but for $l=0$ the terms of order a^2 in γ must be kept, and one then also has to expand the Γ-functions. We give here the resulting expressions for the reaction amplitudes:

$$\left.\begin{aligned}
A'(\theta)&=K\,[1+(-0.1789+i\,\pi/3)\,a^2]\sin\theta\exp(-i\,a\cos\theta),\\
E'(\theta)&=K\,(0.1884-i\,\pi/12)\,a^2\sin\theta,\\
F'(\theta)&=K\,(0.0116+i\,\pi/12)\,a^2\cos\theta,\\
G'(\theta)&=0.
\end{aligned}\right\} \tag{2.4}$$

K is given in (2.2). The decimal numbers in (2.4) are sums of fractional numbers and terms containing Euler's constant (from the logarithmic derivatives of the Γ-functions).

From (2.4) we can compute the various quantities of interest (see I (1.14) to (1.20)). The total cross section to order a^2 is

$$\sigma=\sigma_0\,(1-0.36\,a^2). \tag{2.5}$$

The relative angular distribution of photoelectrons from linearly polarized photons is

$$\sigma(\theta,\phi)\sim\sin^2\theta\cos^2\phi+(0.069+0.035\sin^2\theta)\,a^4. \tag{2.6}$$

(2.6) gives the correct lowest order expression for the term that is independent of $\cos^2\phi$. For unpolarized photons this term should be dropped in a consistent approximation, and in this case we still have the non-relativistic distribution $\sin^2\theta$. The a^4 term gives a small emission of photoelectrons in the plane perpendicular to the polarization plane:

$$\int\sigma(\theta,\tfrac{1}{2}\pi)\sin\theta\,d\theta\Big/\int\sigma(\theta,0)\sin\theta\,d\theta=0.14\,a^4. \tag{2.7}$$

This term also gives the lowest order non-zero forward and backward emission intensity, as the $\cos^2\phi$ term must always vanish for $\theta=0$ and π (cf. I (1.14), (1.7), and (1.8)). We then get for the ratio of forward and backward to maximum emission intensities

$$\sigma(0)/\sigma(\tfrac{1}{2}\pi) = \sigma(\pi)/\sigma(\tfrac{1}{2}\pi) = 0.14\,a^4. \tag{2.8}$$

For the polarizations P_1, P_2, and P_3 (see I (1.17)–(1.20)) we obtain

$$\left.\begin{aligned} P_1 &= -\pi/6\,a^2 \cot\theta, \\ P_2 &= 0.40\,a^2 \cos\theta, \\ P_3 &= 0.40\,a^2 \frac{\sin^2\theta - 0.058}{\sin\theta}. \end{aligned}\right\} \tag{2.9}$$

3. Numerical calculation for $Z = 92$

We have also made numerical calculations of the matrix elements in (1.2) and (1.3) for $Z = 92$ ($a = 0.6715$), taking into account all transitions to final states up to and including $g_{7/2}$ and $g_{9/2}$ ($\varkappa = 4$ and -5). The H_7 functions were calculated from (1.5), where the ${}_1F_1$ functions are obtained from their power series expansions.

The resulting radial multipole moments

$$a'_\varkappa = \lim_{p\to 0} p^{\frac{1}{2}}\, a_\varkappa, \tag{3.1}$$

and similar for $b'_\varkappa$, are given in Table 1. From this table we see that the magnitude of the multipole moments decreases rapidly with increasing multipole order; the $E1$ multipoles are dominant, as could be expected, and next in importance comes $E2$, and then $M2$ and $M1$.

Table 1. Table of radial matrix elements $a'_\varkappa$ and $b'_\varkappa$ (3.1), corresponding to absorption of electric and magnetic multipoles under transition from the initial $1s_{\frac{1}{2}}$ state to final state, specified by $\varkappa$. $Z = 92$, $\beta = 0$.

Transition to final state with $\varkappa$		Electric multipole	$a'_\varkappa$	Magnetic multipole	$b'_\varkappa$
$s_{1/2}$	-1	—	—	$M1$	-0.0106
$p_{1/2}$	1	$E1$	0.0963	—	—
$p_{3/2}$	-2	$E1$	-0.2283	$M2$	0.0136
$d_{3/2}$	2	$E2$	0.0286	$M1$	-0.0017
$d_{5/2}$	-3	$E2$	-0.0390	$M3$	0.0034
$f_{5/2}$	3	$E3$	0.0038	$M2$	-0.0002
$f_{7/2}$	-4	$E3$	-0.0046	$M4$	0.0005
$g_{7/2}$	4	$E4$	0.0004	$M3$	0.0000
$g_{9/2}$	-5	$E4$	-0.0005	$M5$	0.0000

Using the results in Table 1 and the phases obtained from (1.7) we have computed the functions $A'(\theta)$ … $G'(\theta)$, and from this tabulation the cross sections and polarizations can be calculated.

The total cross section is obtained directly from Table 1 and I (3.9), and is

$$\sigma = 0.789\,\sigma_0. \tag{3.2}$$

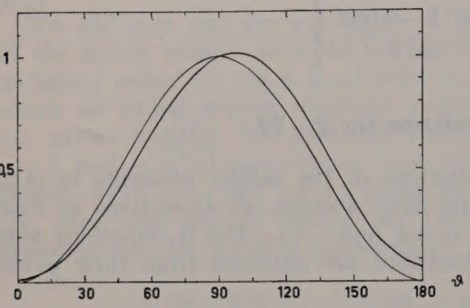

Fig. 1.

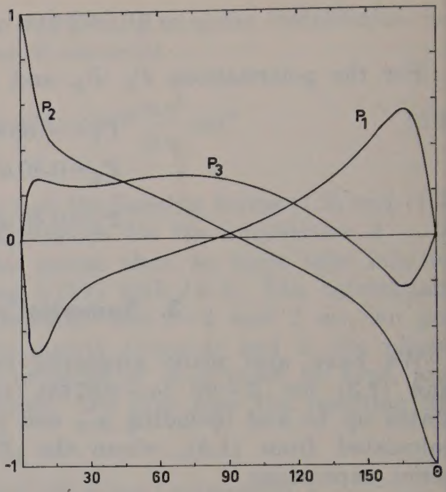

Fig. 2.

Fig. 1. Angular distribution of zero-energy K-shell photoelectrons from $Z=92$. The curve drawn with thin line is the non-relativistic $\sin^2\theta$ distribution. The curves are normalized to one at $\theta=90°$.

Fig. 2. Polarizations of zero-energy K-shell photoelectrons, $Z=92$. P_1 is a transverse polarization perpendicular to the scattering plane, and is obtained also for unpolarized photons, P_2 and P_3 are longitudinal and transverse polarizations in the scattering plane, corresponding to circularly polarized photons.

σ_0 is the non-relativistic value given in (2.3). We thus get a reduction of the cross section with 21 % (the a^2 term in (2.5) gives 16 %), provided we use in both cases the same value for the photon energy $h\nu$. The factor $mc^2/h\nu$ comes from the normalization of the incident photon flux, so it is not entirely inconsistent to use both relativistically and non-relativistically the same (experimental) value, although the theoretical binding energies in a pure Coulomb field are rather different in the Schrödinger and Dirac cases (115 and 132 keV, respectively; the experimental value is 116).

The angular distribution of photoelectrons from unpolarized photons is shown in Fig. 1. The distribution is pushed somewhat towards larger angles (cf. discussion in I, Sect. 6 a), the maximum emission occurring for $\theta=97°$. About 45 % of the photoelectrons are emitted into the forward hemisphere ($\theta<90°$). We also get finite forward and backward intensities, amounting to 1 and 7 %, respectively, of the maximum intensity. The asymmetry around 90° is mainly due to interference between the outgoing p- and d-waves.

If the photons are linearly polarized, we get the value 0.05 for the ratio defined in (2.7).

The electron polarizations are shown in Fig. 2. The degrees of polarization can be rather large, especially for angles near $\theta=0$ and 180°. For large backward angles (around 160°) one obtains, even for unpolarized photons, a transverse polarization of more than 50 %. The lowest order expressions (2.9) give the general trend of the θ-dependence, but the quantitative agreement is in general not very good.

The relative inaccuracy, due mainly to neglect of higher order multipoles, in the numerical results underlying Figs. 1 and 2 is estimated not to exceed a few percent for the polarizations. The angular distribution is probably more accurate, and for the total cross section the contribution from multipoles with $L > 2$ is less than 0.3 %.

The results of this paper should be applied with some care to the actual photoeffect at the K-shell threshold. When the outgoing photoelectron has zero energy one could expect the influence of screening, particularly on the polarizations, to be considerable. The simple screening correction to the total cross section (see e.g. Bethe and Salpeter, 1957, p. 391; this correction assumes that one has an analytical expression for the total cross section near the threshold), which consists in replacing the actual potential in the K-shell region by a displaced Coulomb potential with an effective charge, is hardly applicable to angular distributions and polarizations, as these effects are sensitive to the relative phases of the different partial waves.

ACKNOWLEDGEMENT

We wish to thank Statens Råd för Atomforskning for financial help with the numerical calculations on the electronic computer BESK.

Division of Mathematical Physics, Royal Institute of Technology, and Institute of Theoretical Physics, University of Stockholm.

REFERENCES

BETHE, H., and SALPETER. E. E., 1957. Handbuch der Physik XXXV. (Springer 1957.)
NAGEL, B. C. H., 1960. Arkiv f. Fys. *18* (1960), p. 1.
OLSSON, P. O. M., 1959. Arkiv f. Fys. *15* (1959), pp. 131, 159, 289.
OLSSON, P. O. M., and HULTBERG, S., 1959. Arkiv f. Fys. *15* (1959), p. 361.

Tryckt den 19 maj 1960

Uppsala 1960. Almqvist & Wiksells Boktryckeri AB